BMC Musculoskeletal Disorders

RESEARCH

Open Access

Transcutaneous CO_2 application combined with low-intensity pulsed ultrasound accelerates bone fracture healing in rats

Kenichi Sawauchi[1], Tomoaki Fukui[1], Keisuke Oe[1], Takahiro Oda[1], Ryo Yoshikawa[1], Kyohei Takase[1], Shota Inoue[2], Ryota Nishida[1], Ryosuke Kuroda[1] and Takahiro Niikura[1,3*]

Abstract

Background Low-intensity pulsed ultrasound (LIPUS) is a non-invasive therapy that accelerates fracture healing. As a new treatment method for fracture, we recently reported that the transcutaneous application of CO_2 accelerated fracture healing in association with promoting angiogenesis, blood flow, and endochondral ossification. We hypothesized that transcutaneous CO_2 application, combined with LIPUS, would promote bone fracture healing more than the single treatment with either of them.

Methods Femoral shaft fractures were produced in 12-week-old rats. Animals were randomly divided into four groups: the combination of CO_2 and LIPUS, CO_2, LIPUS, and control groups. As the transcutaneous CO_2 application, the limb was sealed in a CO_2-filled bag after applying hydrogel that promotes CO_2 absorption. Transcutaneous CO_2 application and LIPUS irradiation were performed for 20 min/day, 5 days/week. At weeks 1, 2, 3, and 4 after the fractures, we assessed the fracture healing process using radiography, histology, immunohistochemistry, real-time PCR, and biomechanical assessment.

Results The fracture healing score using radiographs in the combination group was significantly higher than that in the control group at all time points and those in both the LIPUS and CO_2 groups at weeks 1, 2, and 4. The degree of bone fracture healing in the histological assessment was significantly higher in the combination group than that in the control group at weeks 2, 3, and 4. In the immunohistochemical assessment, the vascular densities of CD31- and endomucin-positive microvessels in the combination group were significantly higher than those in the control and LIPUS groups at week 2. In the gene expression assessment, significant upregulation of runt-related transcription factor 2 (Runx2) and vascular endothelial growth factor (VEGF) was detected in the combination group compared to the LIPUS and CO_2 monotherapy groups. In the biomechanical assessment, the ultimate stress was significantly higher in the combination group than in the LIPUS and CO_2 groups.

Conclusion The combination therapy of transcutaneous CO_2 application and LIPUS had a superior effect in promoting fracture healing through the promotion of angiogenesis and osteoblast differentiation compared to monotherapy.

*Correspondence:
Takahiro Niikura
tniikura@med.kobe-u.ac.jp

Full list of author information is available at the end of the article

Keywords Bone, Fracture healing, Carbon dioxide, Transcutaneous CO_2 application, Low-intensity pulsed ultrasound, Combination therapy

Background

Approximately 5–10% of fractures do not heal normally, resulting in delayed union or nonunion [1]. The fracture healing process is complex, and various factors are necessary for successful fracture treatment, including mechanical stability, osteogenic cells, growth factors, scaffolds, and vascularity [2, 3].

The development and clinical application of fracture healing promotion methods can contribute to the early recovery of patients' daily life and social activities and the improvement of their quality of life. Tools currently available in the clinical setting to promote fracture healing include low-intensity pulsed ultrasound (LIPUS) [4], bone morphogenetic proteins treatment [5], and parathyroid hormone treatment [6].

LIPUS is a non-invasive therapy that can accelerate fracture healing through physical stimulation of the area surrounding the fracture. Although the mechanisms of bone healing by LIPUS are not completely understood, nano-motion at the fracture site by LIPUS is converted into biochemical signals via integrin mechanoreceptors [7]. Multiple pathways are induced, primarily cyclooxygenase 2 (COX-2) transcription. As a result of increased intracellular COX-2 production, prostaglandin E2 is then released from cells and activates osteogenic genes through various pathways. Osteogenic genes stimulate endochondral ossification at the fracture area, resulting in accelerated bone remodeling and fracture healing. LIPUS significantly promotes osteoblast differentiation, mainly in mesenchymal stem cells [8, 9], induces angiogenesis, and improves tissue perfusion [10].

We reported the transcutaneous application of CO_2 as a new tool to promote bone fracture healing. Applying the CO_2 absorption-enhancing hydrogel to the skin, CO_2 can dissolve into the gel and pass through the skin to reach deep tissues. We have confirmed that transcutaneous application of CO_2 has tissue regeneration effects, including local tissue oxygenation through the Bohr effect, increased blood flow, and angiogenesis [11, 12]. Previous studies with rat fracture models, rat bone defect models, and rabbit distraction osteogenesis models have shown that transcutaneous CO_2 application promotes bone repair by enhancing angiogenesis, blood flow, and endochondral ossification at the fracture, bone defect, and distraction osteogenesis sites, respectively [13–15].

We hypothesized that transcutaneous CO_2 application combined with LIPUS would promote better bone fracture healing than monotherapy with either of them. In this study, we asked the following questions: (1) Do transcutaneous CO_2 application and LIPUS cancel each other out during combination therapy? (2) Are there additive or synergistic effects of transcutaneous CO_2 application and LIPUS in combination therapies? This study aimed to investigate these questions using the experimental fracture model in rats.

Methods

Animal model

A total of 180 male, 12-week-old Sprague–Dawley rats (SLC Japan, Shizuoka, Japan), weighing an average of 398.2 g (±15.8 g), were used under a research protocol. After the intraperitoneal administration of medetomidine (0.15 mg/kg), midazolam (2 mg/kg), and butorphanol (2.5 mg/kg) for preoperative anesthesia and sedation, we shaved the hairs on the rat's lower limbs. Following a skin incision on the knee, we performed a retrograde insertion of a 1.25 mm diameter K-wire into the femoral intramedullary canal. A standard stabilized closed transverse femoral fracture model was produced by fixing the femur with a three-point bender and dropping weight at the center of the femur [16]. The X-ray image taken immediately after producing the fracture model is shown in Fig. 1. After waking up from anesthesia, weight-bearing restrictions, plaster casts, or other external fixations were not applied. The rats were euthanized using an overdose of pentobarbital for subsequent assessments. This study was approved by the Institutional Animal Care and Use Committee (Permission number: P180609) and carried out in according with the Kobe University Animal Experimentation Regulation. We complied with the ARRIVE guidelines.

Procedure for the transcutaneous CO2 application and LIPUS

Fresh fractured rats were randomly divided into four groups (n=45 in each group, Fig. 2): the combination of CO_2 and LIPUS treatment group (CO_2+LIPUS group), CO_2 treatment group (CO_2 group), LIPUS treatment group (LIPUS group), and sham treatment group (control group). In the CO_2+LIPUS group, we first performed transcutaneous CO_2 application to the fractured lower limbs. After sedation using a minimum dose of isoflurane, we applied the hydrogel, which consisted of carbomer (0.65%), glycerin (5.00%), sodium hydroxide (0.18%), sodium alginate (0.15%), sodium dihydrogen phosphate (0.15%), methylparaben (0.10%), and deionized water (93.77%), to the fractured lower limb and packed it in a polyethylene bag filled with 100% CO_2 for 20 min [13]. LIPUS was applied to the fracture site for 20 min immediately after the CO_2 application. The

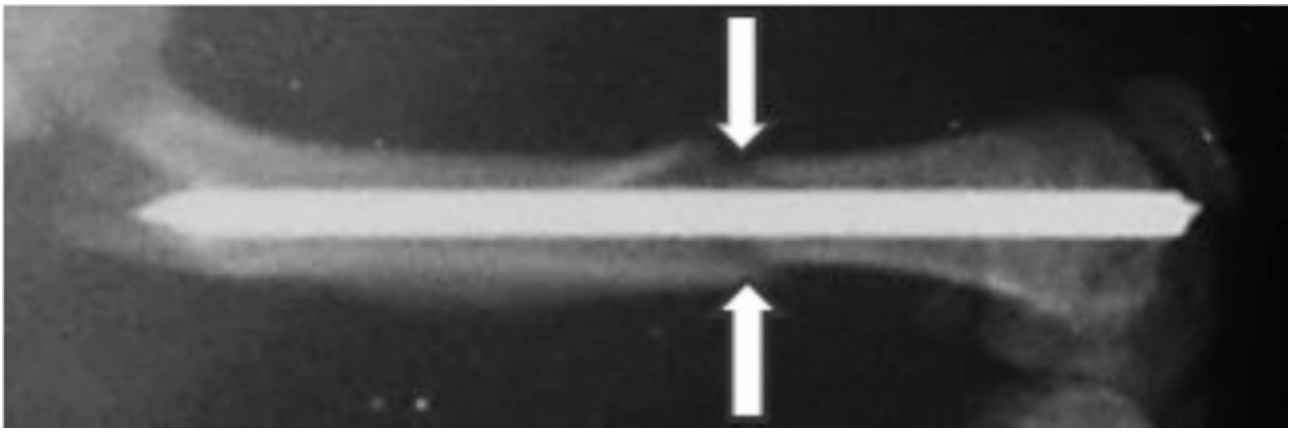

Fig. 1 The X-ray of the femur which was taken immediately after producing the fracture model. White arrows indicate the fracture line

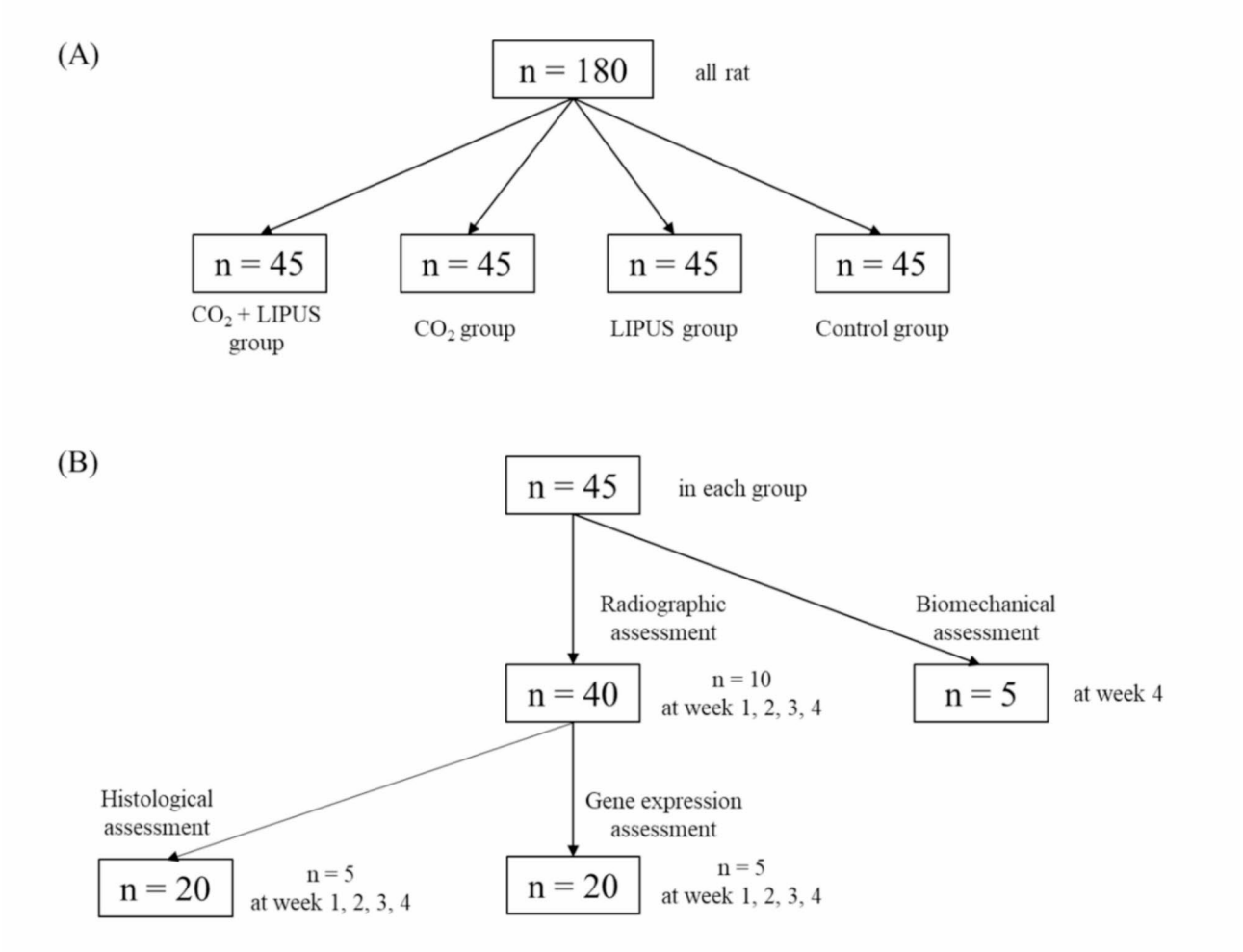

Fig. 2 The study design schema of the number in each group and assessment. (A) 180 rats were randomly divided into four groups ($n = 45$ in each group): the combination of CO_2 and LIPUS treatment group (CO_2 + LIPUS group), CO_2 treatment group (CO_2 group), LIPUS treatment group (LIPUS group), and sham treatment group (control group). (B) Of the 45 rats in each group, 40 rats ($n = 10$ at weeks 1, 2, 3, 4) were used for radiographic assessment and 5 for biomechanical evaluation at week 4. Of the 40 rats for radiographic assessment, 20 rats each were used for histological assessment and gene expression assessment ($n = 5$ at weeks 1, 2, 3, and 4 in each assessment)

parameters of LIPUS are shown in Table 1. In the CO_2 group, we performed CO_2 application only; in the LIPUS group, we performed LIPUS only. Control animals were subjected to sham treatment with air instead of CO_2. The CO_2 and LIPUS treatments were first performed 24 h after fracture creation and were performed five times per week.

Radiographic assessment

At weeks 1, 2, 3, and 4 after the fractures, radiographs of the fractured limbs were obtained ($n=10$ in each group at each time point). Fracture union was diagnosed when bridging callus formation was observed in all four cortices in the anteroposterior and lateral views [17]. In addition, we assessed fracture healing using the Radiographic Union Score for Tibial fracture (RUST) [18], which is a scoring system used to evaluate fracture healing by determining the presence of callus formation and fracture line on the X-ray. A visible fracture line without callus is scored as 1 point, a visible fracture line with callus is scored as 2 points, and a non-visible fracture line with callus is scored as 3 points. The scores are then summed at four locations on the X-ray: anterior, posterior, medial, and lateral. Therefore, RUST ranges from 4 points (no healing) to 12 points (complete healing). RUST was initially used to assess bone healing in human tibial fractures; however, it can also be used in non-human animals and fractures other than the tibia [19]. The inter-examiner error in RUST is reported to be small [20], and it correlates well with the mechanical properties of the fracture site [21]. Three blinded examiners with more than 10 years of clinical experience as orthopedic surgeons assessed fracture union and RUST.

Histological assessment

Fractured femurs were harvested at weeks 1, 2, 3, and 4 ($n=5$ in each group at each time point) and fixed in 4% paraformaldehyde for 24 h at room temperature and demineralized using a demineralization solution that is a 1:1 mixture of 10% formic acid and 10% formalin. After embedding the femurs in paraffin wax, 6-μm sagittal sections were prepared, deparaffinized in xylene, dehydrated in a graded alcohol series, and stained with Safranin-O/Fast Green. Three sections were obtained in each sample. Light microscopy was used to visualize detailed histological structures and cartilage regions. We assessed the degree of fracture healing using the Allen's grading system with a five-point scale (grade 0: nonunion; grade 1: incomplete cartilage union; grade 2: complete cartilage union; grade 3: incomplete bone union; grade 4: complete bone union) [22]. Three blinded examiners with experience in basic research regarding fracture repair scored the degree of fracture healing using the Allen's grading system.

Table 1 LIPUS parameters applied in this experiment

Parameter	Characteristics
Spatial-average temporal-average intensity (mW/cm^2)	30.0
Frequency (MHz)	1.5
Pulse repetition rate (kHz)	1
Pulse duration (μs)	200

Immunohistochemical assessment

We performed an immunohistochemical assessment at week 2 ($n=5$ in each group). We assessed the expression of CD31 and endomucin. CD31 is a specific marker for vascular differentiation [23], and vascular endothelial cells that highly express CD31 and endomucin are known to be deeply involved in bone regeneration and development [24]. The sections were incubated overnight at 4 °C with an anti-CD31 antibody (1:200, Beijing Biosynthesis Biotechnology Co., Ltd., Beijing, China) or anti-endomucin antibody (1:200, Proteintech Group, Inc., Illinois, USA). After washing, the sections were incubated with horseradish peroxidase-labeled anti-mouse (1:200, Nichirei Bioscience, Tokyo, Japan) at room temperature for 60 min. The signal was developed as a brown reaction product using the peroxidase substrate 3, 3-diaminobenzidine (Nichirei Bioscience, Tokyo, Japan). The sections were counterstained with hematoxylin and examined with a BZ-X710 microscope (Keyence Corporation, Osaka, Japan). The vascular area of CD31- or endomucin-positive microvessels in each section was measured in four random fields, and the average was calculated. The percentage of vascular area relative to the total image area was evaluated as the vascular density (%).

Gene expression assessment

We measured the expression of several genes using real-time PCR at weeks 1, 2, 3, and 4 ($n=5$ in each group at each time point). We added TRIzol (Invitrogen, Carlsbad, California, USA) to the callus tissue harvested from around the fracture and homogenized with a T18 ULTRA-TURRAX homogenizer (IKA Werke, Staufen, Germany). Total RNA was extracted by the acid guanidinium thiocyanate-phenol-chloroform method and purified using RNeasy Mini Kit (Qiagen, California, USA) and RNase-free DNase kit (Qiagen). RNA samples were reverse transcribed to single-strand complementary DNA (cDNA) using a high-capacity cDNA reverse transcription kit (Applied Biosystems, Foster City, California, USA). Measurements were performed in duplicates using the Applied Biosystems 7500 real-time PCR system and SYBR Green reagent (Applied Biosystems). All primer sequences are shown in Table 2.

GAPDH, glyceraldehyde-3-phosphate dehydrogenase; MMP-13, matrix metalloproteinase-13; ALP, alkaline phosphatase; Runx2, runt-related transcription factor 2;

Table 2 Details of the primers used for amplification

Gene	Primer sequences (5′ to 3′) (forward/reverse)
GAPDH	AAATGGTGAAGGTCGGTGTG
	TGAAGGGGTCGTTGATGG
Collagen II	GGGCTCCCAGAACATCACCTACCA
	TCGGCCCTCATCTCCACATCATTG
Collagen X	GGCAGCAGCACTATGACCCAA
	ACAGGCCTACCCAAACGTGAGTCC
MMP-13	CCCTGGAGCCCTGATGTTT
	CTCTGGTGTTTTGGGGTGCT
ALP	TCCCAAAGGCTTCTTCTTGC
	ATGGCCTCATCCATCTCCAC
Runx2	GCGTCAACACCATCATTCTG
	CAGACCAGCAGCACTCCATC
Osterix	AGCTCTTCTGACTGCCTGCCTA
	TGGGTGCGCTGATGTTTGCT
VEGF	TGCACTGGACCCTGGCTTTAC
	CGGCAGTAGCTTCGCTGGTAG
eNOS	GACCCTCACCGATACAACATAC
	CATACAGGATAGTCGCCTTCAC
TSP-1	GAGTGTCACTGCCAGAACTCA
	GTCTGTACTGAAGAGCCCTCA

VEGF, vascular endothelial growth factor; eNOS, endothelial nitric oxide synthase; TSP-1, thrombospondin-1.

We assessed the chondrogenic differentiation by measuring the gene expression levels of collagen II, collagen X, and matrix metalloproteinase-13 (MMP-13). To evaluate the osteogenic differentiation, we used alkaline phosphatase (ALP), runt-related transcription factor 2 (Runx2), and osterix. We also examined the following genes: vascular endothelial growth factor (VEGF), which is the angiogenic factor; endothelial nitric oxide synthase (eNOS), which is involved in vasodilation [25]; and thrombospondin-1 (TSP-1), which is an angiogenesis inhibitor [26].

Each gene's expression levels were compared relative to that of glyceraldehyde-3-phosphate dehydrogenase, which was used as the housekeeping gene. The ΔΔCT method was used to quantify gene expression as fold change relative to one of the samples in the control group at week 1 [27].

Biomechanical assessment

A three-point bending test was performed on the femoral shaft at week 4 ($n=5$ in each group) using a bone strength measurement device, MZ500S (Maruto, Tokyo, Japan). The front surface of the femur was placed upward, and a load of 500 N was applied from above at a speed of 5 mm/min to the fracture site. The ultimate stress (N), extrinsic stiffness (N/mm), and failure energy (N · mm) were computed from the measurement results. The ratio of each parameter of the fractured femur to that in the left femur, which was the healthy limb of the same rat, was calculated.

Statistics analysis

Fisher's exact test, followed by the post hoc Bonferroni test, was used to compare the fracture union rate between groups at each time point on the radiographs. The Kruskal–Wallis test with Steel–Dwass post hoc test was used to compare RUST on radiographic assessment, the Allen's grading score on the histological assessment, immunohistochemical assessment, gene expression results, and biomechanical results between the groups at each time point. Statistical significance was set at $P<0.05$. Columns and error bars represent mean and standard error.

Results

Radiographic assessment

Representative radiographs are shown in Fig. 3A. At week 1, no periosteal callus formation on radiographs was observed in the control group, while periosteal callus formation was found in 1–2 of the four cortical bones in the LIPUS and CO_2 groups. In the CO_2+LIPUS group, periosteal callus formation was observed in two of the four cortical bones in most cases. At week 2, all groups showed enlargement of the callus formation; however, none in the control groups showed bridging callus in all four locations. The fracture union rate in the CO_2+LIPUS group was 80%, significantly higher than that of the control group (Table 3). At week 3, fracture union was achieved in all rats in the CO_2 and CO_2+LIPUS groups, and the fracture union rates in both groups were significantly higher than that in the control group (30%). At week 4, fracture union was observed in all rats.

The RUST results are shown in Fig. 3B. The CO_2+LIPUS group had significantly higher scores than the control group at all time points (control at week 1: 4.20±0.13, CO_2+LIPUS at week 1: 6.10±0.18, $P<0.001$; control at week 2: 5.70±0.30, CO_2+LIPUS at week 2: 8.20±0.13, $P<0.001$; control at week 3: 7.00±0.37, CO_2+LIPUS at week 3: 9.70±0.37, $P=0.0014$; control at week 4: 10.10±0.38, CO_2+LIPUS at week 4: 12.00±0.00, $P=0.0011$), and significantly higher scores than the LIPUS and CO_2 groups at weeks 1, 2, and 4 (LIPUS at week 1: 4.70±0.21, $P=0.0035$; CO_2 at week 1: 4.80±0.20, $P=0.0037$; LIPUS at week 2: 6.90±0.23, $P=0.0034$; CO_2 at week 2: 7.30±0.21, $P=0.018$; LIPUS at week 4: 10.50±0.40, $P=0.0093$; CO_2 at week 4: 11.00±0.21, $P=0.0029$). At weeks 2 and 3, the CO_2 group scored higher than the control group (at week 2: $P=0.0073$; CO_2 at week 3: 9.00±0.26, $P=0.0046$), and the LIPUS group at week 2 scored higher than the control group ($P=0.046$).

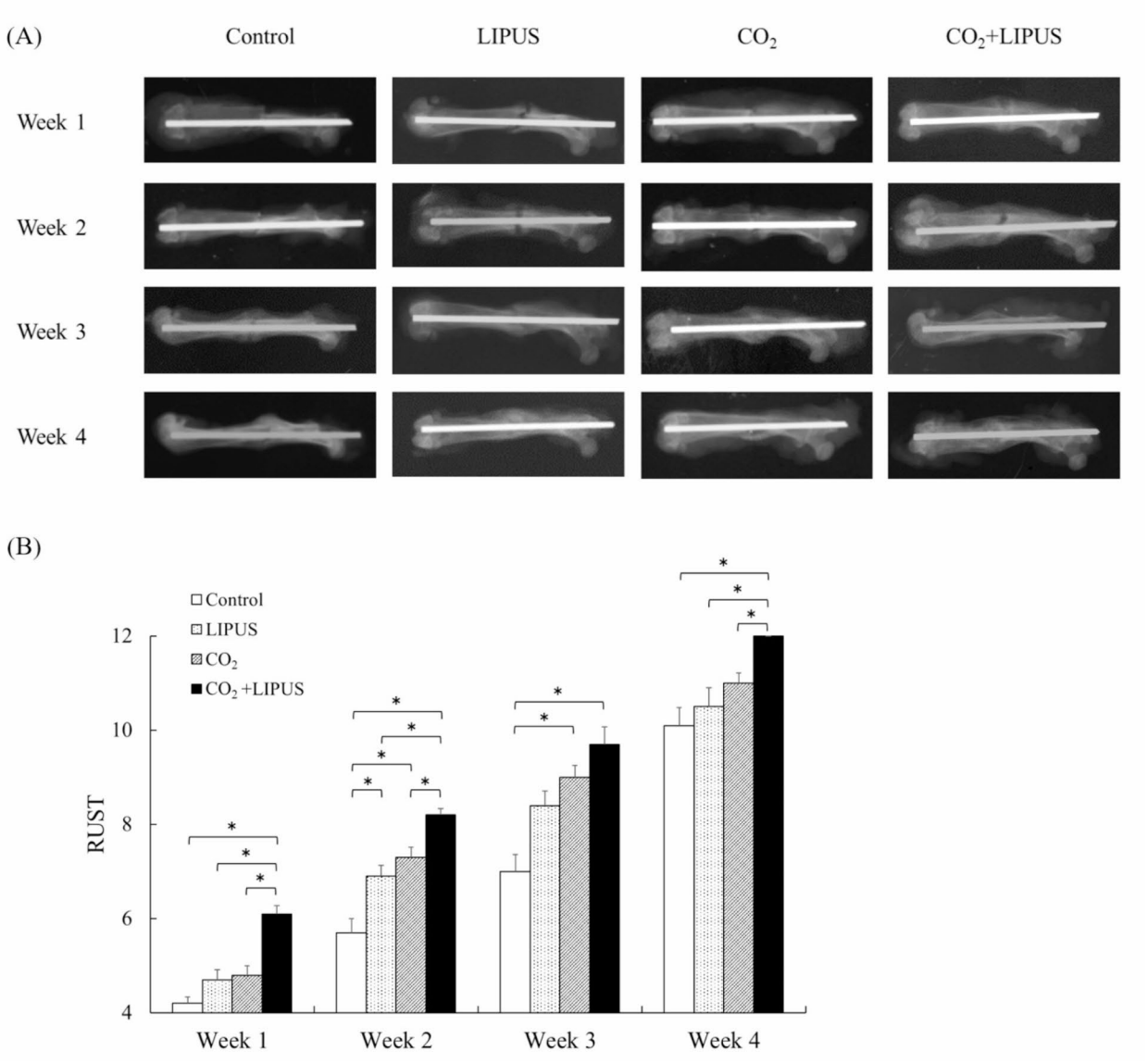

Fig. 3 Radiographic assessment in each group at each time point. (A) Representative radiographs of each group, at each time point are shown. At week 1, there was no periosteal callus formation in control group, while periosteal callus formation was found in one to two of the four cortical bones in anterior, posterior, medial, and lateral sides in LIPUS and CO_2 groups. In the CO_2 + LIPUS group, periosteal callus formation was found in two of the four cortical bones in most cases. At week 2, all groups showed enlargement of the callus formation, however, none of the control group showed bridging callus in all four locations. At week 3, bone healing was achieved in all rats in CO_2 and CO_2 + LIPUS groups. At week 4, bone healing was obtained in all rats. (B) The graph showed the degree of fracture repair evaluated by the Radiographic Union Score for Tibial fracture (RUST) in control, LIPUS, CO_2, and CO_2 + LIPUS groups at each time point ($n = 10$ in each group). The CO_2 + LIPUS group had significantly higher scores than the control group at all time points and significantly higher than LIPUS and CO_2 groups at weeks 1, 2, and 4. At weeks 2 and 3, the CO_2 group was higher than the control group, and the LIPUS group at week 2 was higher than the control group (*: $P \leq 0.05$)

The CO_2 + LIPUS group showed bridging callus and disappearance of the fracture lines in all cases at week 4.

At week 2, the fracture union rate in the CO_2 + LIPUS group was significantly higher than in the control group. At week 3, the fracture union rates in CO_2 + LIPUS and CO_2 groups were significantly higher than in the control group.

Histological assessment

Representative histological images are shown in Fig. 4A. Cartilage formation in the woven bone was observed in all groups, particularly in the CO_2 + LIPUS group at week (1) Cartilage union was observed in some samples from the CO_2 and CO_2 + LIPUS groups at week (2) There was little cartilage in the CO_2 + LIPUS group at week 3, indicating that endochondral ossification was progressing. At week 4, there was little cartilage even in the control

Table 3 Fracture union rate in each group at each time point

	Control	LIPUS	CO_2	CO_2+LIPUS	*P* value
Week 1	0/10 (0%)	0/10 (0%)	0/10 (0%)	0/10 (0%)	ns
Week 2	0/10 (0%)	2/10 (20%)	4/10 (40%)	8/10 (80%)	0.0043 (control –CO_2+LIPUS)
Week 3	3/10 (30%)	7/10 (70%)	10/10 (100%)	10/10 (100%)	0.019 (control –CO_2+LIPUS) 0.019 (control – CO_2)
Week 4	10/10 (100%)	10/10 (100%)	10/10 (100%)	10/10 (100%)	ns

group, and bone healing was observed in the other three groups. The results of the Allen's grading system scores are shown in Fig. 4B. The Allen's grading system scores were significantly higher in the CO_2+LIPUS group than those in the control group at weeks 2, 3, and 4 (control at week 2: 1.00±0.00, CO_2+LIPUS at week 2: 2.20±0.20, P=0.020; control at week 3: 1.93±0.07, CO_2+LIPUS at week 3: 3.60±0.24, P=0.031; control at week 4: 3.40±0.16, CO_2+LIPUS at week 4: 4.00±0.00, P=0.024). They were significantly higher in the LIPUS and CO_2 groups than in the control group at week 3 (LIPUS at week 3: 2.80±0.13, P=0.032; CO_2 at week 3: 3.00±0.11, P=0.032).

Immunohistochemical assessment

Representative immunohistochemical images are shown in Fig. 5A. The vascular densities of CD31-positive microvessels were significantly higher in the LIPUS, CO_2, and CO_2+LIPUS groups than those in the control group (control: 2.33±0.47%; LIPUS: 4.05±0.29%, P=0.045; CO_2: 6.62±0.52%, P=0.045; CO_2+LIPUS: 7.45±0.66%, P=0.045), and those in CO_2 and CO_2+LIPUS groups were also higher than in the LIPUS group (CO_2: P=0.045; CO_2+LIPUS: P=0.045) (Fig. 5B). The vascular density of endomucin-positive microvessels in CO_2+LIPUS was higher than in the control and LIPUS group (control: 0.70±0.22%, P=0.045; LIPUS: 0.87±0.24%, P=0.045; CO_2+LIPUS: 3.44±0.63%), and that in the CO_2 group was higher than in the control group (CO_2: 3.00±0.49%, P=0.045) (Fig. 5C).

Gene expression assessment

Gene expression levels in tissues around the fracture sites assessed by real-time PCR are shown in Fig. 6.

As for genes related to chondrogenic differentiation, gene expression of collagen II was significantly higher in the CO_2+LIPUS group than in the control group at weeks 1 and 2 (control at week 1: 1.02±0.86, CO_2+LIPUS at week 1: 5.44±0.81, P=0.045; control at week 2: 3.09±0.79, CO_2+LIPUS at week 2: 14.01±0.72, P=0.045), and significantly higher in the CO_2 group than in the control group at week 2 (CO_2 at week 2: 12.50±0.77, P=0.045). Collagen X expression was higher in the CO_2+LIPUS group than in the control and LIPUS groups at week 2 (CO_2+LIPUS: 117.30±1.60; control: 32.99±0.68, P=0.045; LIPUS: 39.12±0.61, P=0.045). The gene expression of MMP-13 was significantly higher in the CO_2 and CO_2+LIPUS groups than in the control group at week 3 (control: 6.40±0.82; CO_2: 16.68±0.71, P=0.045; CO_2+LIPUS: 18.64±0.83, P=0.045).

Regarding genes related to osteoblast differentiation, the expression of ALP at weeks 2 and 3 was higher in the CO_2 and CO_2+LIPUS groups than in the control group (control at week 2: 0.82±0.62; CO_2 at week 2: 2.89±1.08, P=0.045; CO_2+LIPUS at week 2: 3.28±1.42, P=0.045; control at week 3: 1.78±0.69; CO_2 at week 3: 5.32±0.86, P=0.045; CO_2+LIPUS at week 3: 7.04±1.04, P=0.045). Runx2 expression in the CO_2+LIPUS group was higher than those in the control and LIPUS groups at weeks 2 and 3 (CO_2+LIPUS at week 2: 8.11±1.15; control at week 2: 1.33±0.83, P=0.045; LIPUS at week 2: 3.13±0.58, P=0.045; CO_2+LIPUS at week 3: 10.84±0.59; control at week 3: 2.49±0.52, P=0.045; LIPUS at week 3: 4.81±0.55, P=0.045), and higher than in the CO_2 group at week 3 (CO_2 at week 3:5.83±0.66, P=0.045); at week 2, the CO_2 group showed a higher expression than the LIPUS group (CO_2 at week 2:7.88±0.69, P=0.045). The osterix levels in the LIPUS and CO_2+LIPUS groups were significantly higher than in the control group at week 3 (control: 9.15±0.66; LIPUS: 17.65±0.66, P=0.045; CO_2+LIPUS: 19.19±0.94, P=0.045).

The gene expression of VEGF was significantly higher in the LIPUS, CO_2, and CO_2+LIPUS groups than those in the control group at all time points (control at week 1: 1.30±0.91; LIPUS at week 1: 3.18±0.57, P=0.045; CO_2 at week 1: 3.33±0.54, P=0.045; CO_2+LIPUS at week 1: 4.41±0.76, P=0.045; control at week 2: 2.29±0.86; LIPUS at week 2: 7.38±0.52, P=0.045; CO_2 at week 2: 6.50±0.59, P=0.045; CO_2+LIPUS at week 2: 12.71±0.76, P=0.045; control at week 3: 5.68±1.00; LIPUS at week 3: 21.74±0.63, P=0.045; CO_2 at week 3: 27.51±1.26, P=0.045; CO_2+LIPUS at week 3: 44.32±1.38, P=0.045; control at week 4: 1.41±0.66; LIPUS at week 4: 4.34±0.60, P=0.045; CO_2 at week 4: 4.91±0.73, P=0.045; CO_2+LIPUS at week 4: 5.54±0.74, P=0.045), and was also higher in the CO_2+LIPUS group than those in the LIPUS and CO_2 groups at week 2 (LIPUS: P=0.045; CO_2: P=0.045). The gene expression of eNOS at week 2 was higher in the CO_2+LIPUS group than in the control and LIPUS groups (CO_2+LIPUS: 6.65±1.03; control: 1.72±0.63, P=0.045; LIPUS: 1.87±0.60, P=0.045). There were no significant differences in TSP-1 expression levels among the groups at any time point.

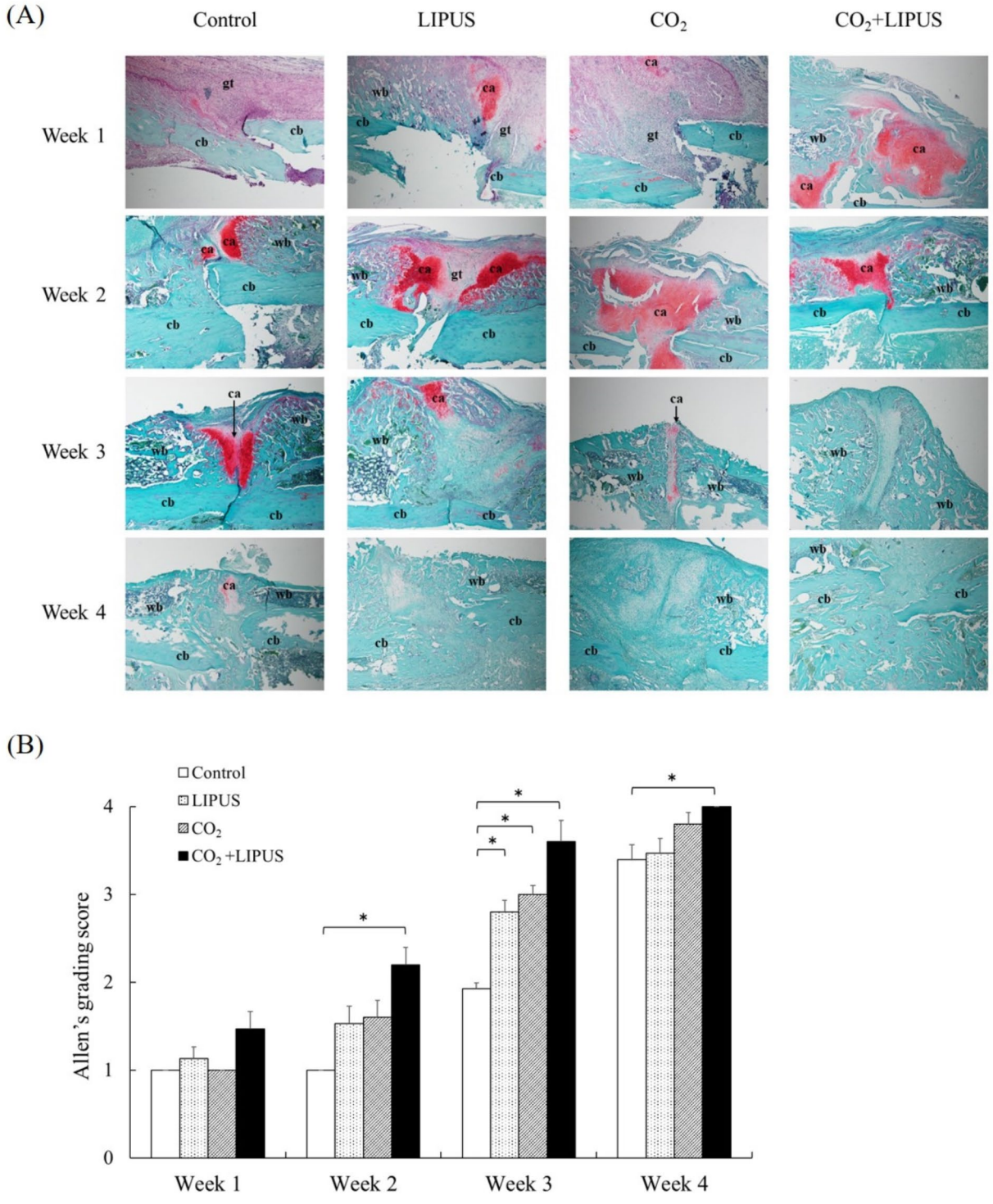

Fig. 4 Histological assessment in each group at each time point. (A) Representative histological sections stained with safranin-O/fast green are shown. At week 1, cartilage formation in the woven bone was observed in all groups, especially in the CO_2 + LIPUS group. At week 2, cartilage union was observed in some samples of CO_2 and CO_2 + LIPUS groups, and at week 3, there was little cartilage in the CO_2 + LIPUS group, indicating that endochondral ossification was progressing. At 4 weeks, there was only little cartilage in the control group, and bone healing was observed in the other three groups. Ca = cartilage; cb = cortical bone; gt = granulation tissue; wb = woven bone. (B) The degree of fracture repair evaluated by Allen's grading score at each time points are shown ($n = 5$ in each group). The score was significantly higher in the CO_2 + LIPUS group than in the control group at weeks 2, 3, and 4, and significantly higher in LIPUS and CO_2 groups than in the control group at week 3 (*: $P \leq 0.05$)

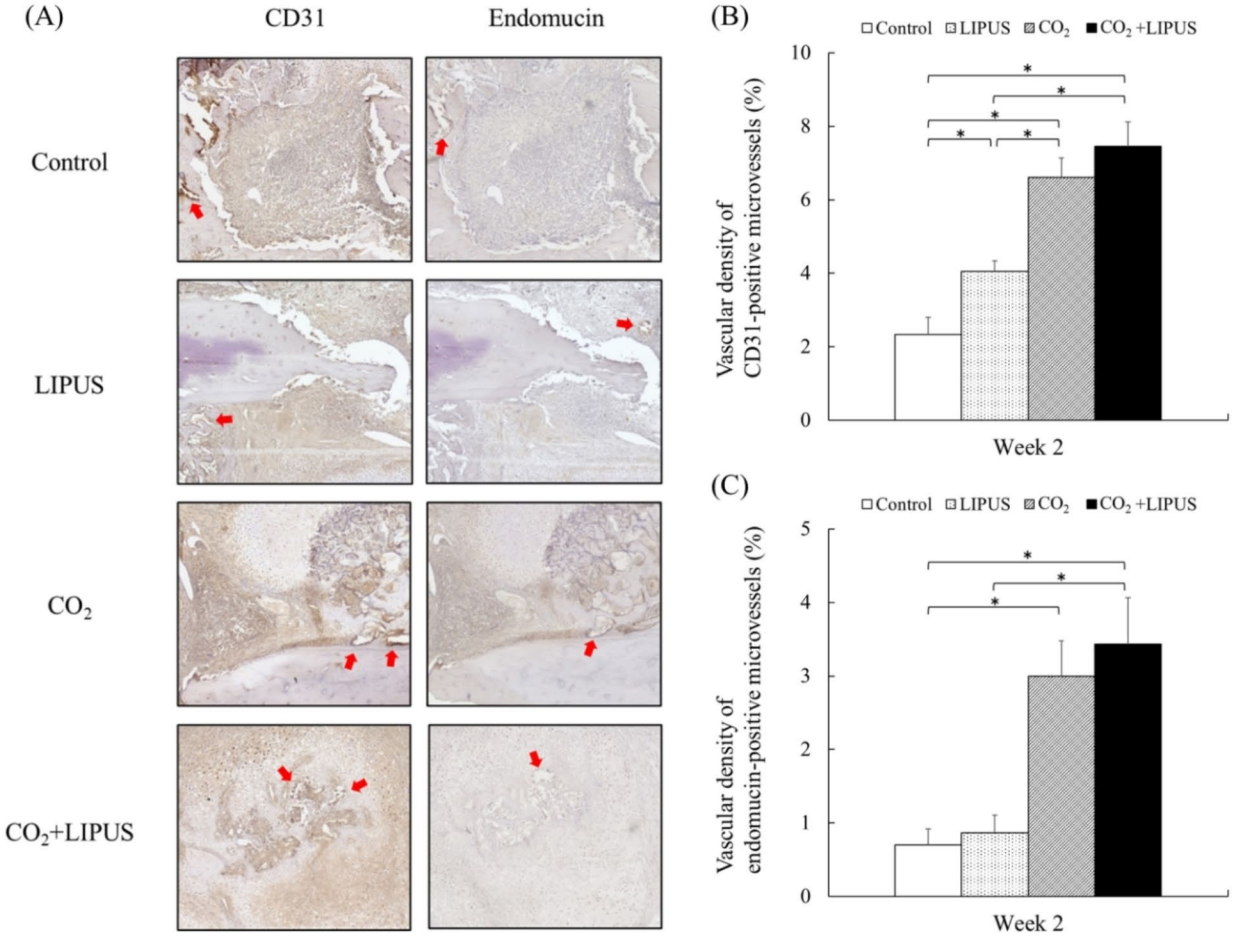

Fig. 5 Immunohistochemical assessment in each group at week 2. (A) Representative images of the immunohistochemical staining for CD31 and endomucin are shown. Red arrows indicate CD31- or endomucin-positive microvessels. (B) The vascular density of CD31-positive microvessels is shown. The vascular density of CD31-positive microvessels was significantly higher in the LIPUS, CO_2, and CO_2 + LIPUS groups than in the control group, and those in the CO_2 and CO_2 + LIPUS groups were higher than those in the LIPUS group. (C) The vascular density of endomucin-positive microvessels is shown. The vascular density of endomucin-positive microvessels in the CO_2 + LIPUS group was higher than that in the control and LIPUS groups, while the CO_2 group showed a higher vascular density compared to that in the control group (*: $P \leq 0.05$).

Biomechanical assessment

The three biomechanical assessment parameters at week 4 are shown in Fig. 7. The ultimate stress and extrinsic stiffness were significantly higher in the LIPUS, CO_2, and CO_2+LIPUS groups than those in the control group (ultimate stress in control: 27.7±3.4%; ultimate stress in LIPUS: 62.9±4.0%, P=0.045; ultimate stress in CO_2: 49.0±3.3%, P=0.045; ultimate stress in CO_2+LIPUS: 80.2±5.9%, P=0.045; extrinsic stiffness in control: 18.6±2.3%; extrinsic stiffness in LIPUS: 56.9±10.8%, P=0.045; extrinsic stiffness in CO_2: 45.0±4.6%, P=0.045; extrinsic stiffness in CO_2+LIPUS: 62.8±12.8%, P=0.045). The ultimate stress was also higher in the CO_2+LIPUS group than in the LIPUS (P=0.045) and CO_2 groups (P=0.045). The failure energy was higher in the CO_2+LIPUS group than in the control group (control: 22.1±2.9%, CO_2+LIPUS: 64.4±13.8%, P=0.045).

Discussion

LIPUS therapy is a non-invasive treatment that can shorten the bone healing period by mechanical stimulation of the fracture site with pulsed ultrasound waves emitted from a probe on the body surface. The promotion of fracture healing has been proven in rat and rabbit fracture models [28, 29], and LIPUS has been shown to be effective throughout the fracture healing process, including the inflammation, reparative, and remodeling phases [30]. LIPUS enhances the gene expression of ALP and Runx2 in rat bone marrow-derived stromal cells [8], accelerates osteoblast differentiation [9], increases the expression of osterix in ROS17/2.8, a rat osteoblast-like cell line [31], and upregulates VEGF expression around the fracture area in a rat fracture model [32]. It has also been reported to promote the expression of collagen II in human chondrocytes [33] but reduce the expression of

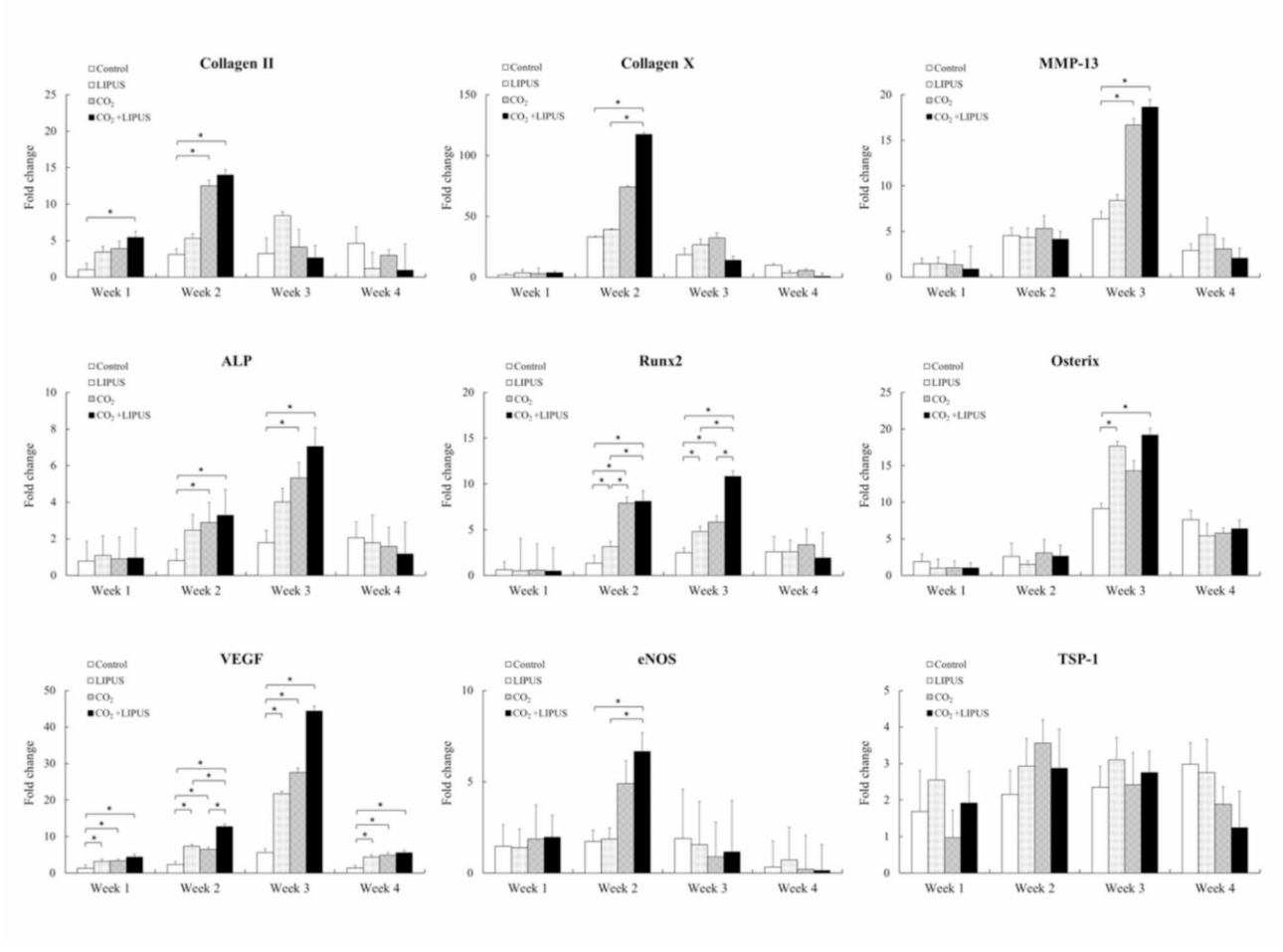

Fig. 6 Expression of the nine genes of interest in each group at each time point. This figure shows the mean expression with standard error of the nine genes of interest in each group at each time point, as measured by quantitative real-time PCR ($n = 5$ in each group). Gene expression levels were normalized to GAPDH and are presented as fold change relative to a sample of the control group at week 1. GAPDH; glyceraldehyde-3-phosphate dehydrogenase, MMP-13; matrix metalloproteinase-13, ALP; alkaline phosphatase, Runx2; runt-related transcription factor 2, VEGF; vascular endothelial growth factor, eNOS; endothelial nitric oxide synthase, TSP-1; thrombospondin-1 (*: $P \leq 0.05$)

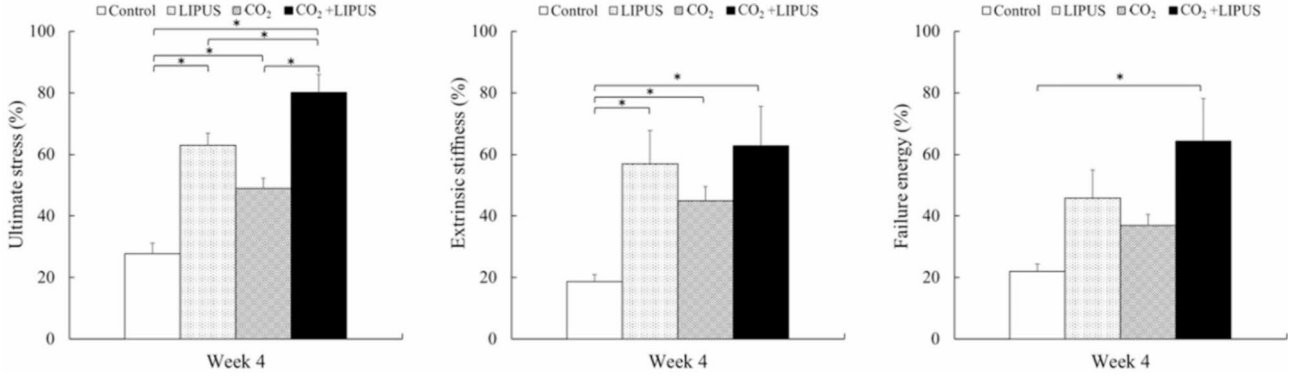

Fig. 7 Biomechanical assessment for fracture repair with three-point bending test in each group at week 4. Here, $n = 5$ in each group. Ultimate stress and extrinsic stiffness were significantly higher in LIPUS, CO_2, and CO_2 + LIPUS groups than in the control group. Ultimate stress was also higher in the CO_2 + LIPUS group than in the LIPUS and CO_2 groups, respectively. Failure energy was higher in the CO_2 + LIPUS group than in the control group (*: $P \leq 0.05$)

MMP-13, which is necessary for normal bone regeneration through proper resorption of hypertrophic cartilage and endochondral ossification [34]. On the other hand, CO_2 therapy has been reported to be effective in treating a variety of pathological conditions. Carbonated springs have long been applied to the treatment of peripheral arterial disease as they are expected to increase blood flow [35]. In recent years, transcutaneous application of CO_2 has been used to treat wounds such as bedsores and skin ulcers [36]. We have designed a system for local absorption of CO_2 through the skin using a hydrogel in which CO_2 is readily dissolved and reported that transcutaneous application of CO_2 has a tissue regenerative effect via local tissue oxygenation by the Bohr effect, which is expressed as a shift in the oxygen dissociation curve of hemoglobin with pH and CO_2 concentration, increased blood flow, and angiogenesis [12]. We have also demonstrated that transcutaneous application of CO_2 promotes bone healing in normal and diabetic rat fracture models [13, 37] and concluded that this is achieved by increasing angiogenesis, promoting endochondral ossification, and differentiating osteoblasts. There are only a few reports on combination therapy to promote fracture healing [38, 39]. To our knowledge, this is the first report on the combination therapy of transcutaneous CO_2 application and LIPUS. In this study, the combination of transcutaneous CO_2 application and LIPUS treatment was superior to the control in all assessments. In addition, the combination therapy had a significantly higher score on the radiographic evaluation of RUST at weeks 1, 2, and 4, gene expression of VEGF at week 2 and Runx2 at week 3 on real-time PCR, and ultimate stress at week 4 on mechanical evaluation than monotherapy. In summary, these results indicate that transcutaneous CO_2 application in combination with LIPUS can accelerate fracture healing.

Radiographic assessment of the combination group showed early callus formation at week 1, bridging callus formation in the four cortical bones in 80% of samples at week 2 and in all samples at week 3, and complete disappearance of the fracture lines in all week 4 samples. In contrast, in the LIPUS or CO_2 monotherapy groups, callus formation began at week 2 in most samples, callus bridging in all four cortices was not obtained in some samples at week 3, and callus bridging was completed at week 4, although the fracture lines did not completely disappear. In the control group, there were no samples of callus bridging in all of the four bone cortices at week 2, and only 30% at week 3 achieved bone union. As with monotherapy, callus bridging was observed at week 4, but the fracture lines did not completely disappear. Only the combined group at weeks 2, 3, and the CO_2 monotherapy group at week 3 showed significant differences in fracture union rates from the control group. RUST demonstrated significantly higher scores in the combination therapy group than in the other three groups at weeks 1, 2, and 4. At week 3, the combination group and CO_2 monotherapy group showed significant differences from the control group, whereas the LIPUS monotherapy group showed no difference. These radiographic results indicated that combination therapy significantly accelerated fracture healing compared to monotherapy at most time points. In addition, the femurs treated with combination therapy were mechanically stronger than those treated with monotherapies, as the combination therapy outperformed the monotherapies at week 4 of ultimate stress. The Allen's grading system scores in histological evaluation showed that combination therapy had comparable or better scores than monotherapies at all time points, although no significant differences between monotherapies and combination therapy were observed. In the combination therapy, the vascular density at week 2 in the immunohistochemical assessment was higher than that in the control and LIPUS monotherapy, and was equal to or higher than that in CO_2 monotherapy.

The fracture healing process consists of three stages: the inflammatory phase, the reparative phase, and the remodeling phase, in which various types of cells cooperate to repair the tissue [40]. In the inflammatory phase, a hematoma formed after the fracture fills the defect between the bone fragments, and is infiltrated by inflammatory and mesenchymal cells [41]. Local oxygen deprivation due to vascular injury stimulates the expression of hypoxia-inducible factor (HIF), which induces the expression of VEGF, which plays an important role in angiogenesis and blood flow and is essential for fracture repair [42, 43]. It has been reported that LIPUS causes an increased VEGF expression through nitric oxide and HIF 1-alpha [44], and VEGF is induced by acidosis in cells around the fracture site [45]. It has been previously reported that transcutaneous CO_2 application caused oxygen dissociation from hemoglobin due to the Bohr effect and a decrease in local pH in the human extremities [12]. In the current study, VEGF expression was upregulated in the combination therapy group compared to that in the control group at all time points and in either monotherapy with LIPUS or CO_2 at week 2. These results suggest that the combination of LIPUS and CO_2 treatments has a superior effect in stimulating VEGF expression compared to monotherapies. eNOS is involved in vasodilation and osteoblast maturation and is upregulated by increased blood flow and VEGF [46, 47]. In this study, the gene expression of eNOS at week 2 was higher in the combination therapy group than in the control and LIPUS groups, although there was no significant difference between the LIPUS and CO_2 groups. Furthermore, immunohistochemical assessments revealed that the vascular densities of CD31- and endomucin-positive

microvessels were higher in the CO_2 and combination groups than in the control group, and those in the combination group were higher than those in the LIPUS group. Cells with high expression of CD31 and endomucin are specific to type H vessels [24], which can induce bone formation. Adding CO_2 application to LIPUS treatment resulted in a significant difference from the control group, indicating that transcutaneous CO_2 application increased the type H vessels in the fracture model. These results suggest that the addition of CO_2 transcutaneous application could accelerate fracture repair promotion by LIPUS through vasodilation and osteoblast maturation and activation.

In the reparative phase, undifferentiated mesenchymal cells, osteoblast progenitor cells, and new blood vessels that are induced in the injured area begin to repair the damaged area. In the deep area under the periosteum and bone marrow with inadequate blood supply and low oxygen concentration, osteoblast progenitor cells are not induced, and chondrocytes appear. In the early stages of chondrogenesis during the reparative phase, mesenchymal stem cells form a chondrogenic matrix containing collagen II. The chondrogenic matrix proliferates and the center of the matrix differentiates into chondrocytes. After the formation of the cartilage matrix, collagen II expression decreases, collagen X expression increases, and chondrocytes mature into hypertrophic chondrocytes [48]. In our study, only the combined treatment group showed a significantly higher expression of collagen II than the control group at week 1, and the combination and CO_2 alone groups had higher expression than the control group at week 2. As for collagen X, the combined treatment group had significantly higher expression than the LIPUS and control groups at week 2. These results of real-time PCR were consistent with those of histological evaluation in that higher Allen's grading system scores were obtained in the combined therapy group than in the control group at all time points except week 1, and those in both monotherapies exceeded the control group only at week 3. The statistically significant difference between the combination therapy and either monotherapy was small; however, it could be interpreted that these results indirectly demonstrated a superior chondrogenic differentiation accelerating effect in the combination therapy to not only the control groups but also monotherapies. MMP-13 is involved in proper resorption of hypertrophic cartilage and is essential for endochondral ossification [49]. It has been reported that MMP-13 is upregulated by transcutaneous CO_2 application in bone fractures of diabetic rats [37] and downregulated by LIPUS in a rabbit knee osteoarthritis model [50]. In our study, MMP-13 expression at week 3 was higher in the combination and LIPUS groups than in the control group, and it was not significantly downregulated by LIPUS. The reason why no negative influence on MMP-13 expression by LIPUS was detected might be that the animal model of the current study was not an osteoarthritis model or that Runx2, which is reported to increase MMP-13 expression [51], was upregulated by LIPUS and transcutaneous CO_2 application. At least, LIPUS did not interfere with the increasing effect of CO_2 on MMP-13 expression in the current study.

ALP and Runx2 are early-stage, and osterix is late-stage osteogenic markers, all playing essential roles in osteoblast differentiation and bone formation [52]. The gene expression levels of ALP and Runx2 demonstrated significant differences among the groups at weeks 2 and 3. As for ALP at weeks 2 and 3, the combination therapy and CO_2 alone groups showed significantly higher expression than the control group. Regarding Runx2, the combination and CO_2 alone groups had higher expression than the other two groups at week 2, and the combination group significantly exceeded all three other groups at week 3. This suggests that combination therapy and CO_2 alone significantly promoted osteoblast differentiation more than the other two groups up to week 2; at week 3, combination therapy promoted differentiation more than CO_2 alone. The gene expression levels of osterix were also higher in the combination therapy group at week 3, and there was no significant difference among the three groups other than the control group. The gene expression assessment suggests that combination therapy upregulates angiogenesis early in the healing process and osteogenesis in the middle to late stages by promoting osteoblast differentiation, resulting in accelerated fracture healing.

The parameters used in LIPUS treatment (1.5 MHz; 200 μs burst width sine wave, with a repeating pulse at 1 kHz; and a spatial and temporal average intensity of 30 mW/cm^2) are the irradiation conditions approved by the U.S. Food and Drug Administration in 1994 as a treatment for promoting healing of fresh fractures. In studies on the spatial and temporal average intensity, it was reported that LIPUS at 30 mW/cm^2 promoted fracture healing more than LIPUS at 150 mW/cm^2 in a rat femur fracture model [53] and that high-intensity ultrasound inhibited bone healing, whereas low-intensity ultrasound stimulated bone repair [54]. Regarding the frequency, it has been reported that LIPUS at 1.5 MHz accelerated the healing of rat femoral fractures more than LIPUS at 0.5MHz [55]. The parameters applied in our experiment are used in most clinical and preclinical studies.

Although not the main purpose of this study, a direct comparison between transcutaneous CO_2 application and LIPUS treatment showed a significant difference only in the gene expression during osteoblast differentiation. Therefore, it can be inferred that there was no significant

difference between these two monotherapies in terms of promoting fracture healing.

This study has some limitations. First, in this study, the effects were only assessed using male rats, and the results might be different if female rats or other animals were used. Second, transcutaneous CO_2 application and LIPUS could not be performed simultaneously because of procedural difficulties. In terms of clinical application, the combination treatment used in this study requires a long intervention time of 40 min per day, which might be a heavy burden for patients. It is possible that combination therapy can be performed simultaneously in larger animals; however, further studies are needed. In addition, since we did not perform the same experiment with the reversed order of CO_2 and LIPUS application, the results in that case are unknown.

Conclusions

The combination therapy of transcutaneous CO_2 application and LIPUS had a superior effect in promoting fracture healing through the promotion of angiogenesis and osteoblast differentiation compared to the monotherapies. More research on the mechanisms of transcutaneous CO_2 application and animal-to-human translational studies are needed before it can be used in clinical practice in the future. However, the combination of transcutaneous CO_2 application and LIPUS has the potential to accelerate fracture healing and may be more beneficial to patients than monotherapy.

Abbreviations

ALP	alkaline phosphatase
COX-2	cyclooxygenase 2
eNOS	endothelial nitric oxide synthase
HIF	hypoxia-inducible factor
LIPUS	low-intensity pulsed ultrasound
MMP-13	matrix metalloproteinase-13
Runx2	runt-related transcription factor 2
RUST	Radiographic Union Score for Tibial fracture
TSP-1	thrombospondin-1
VEGF	vascular endothelial growth factor

Acknowledgements

We thank M. Nagata, M. Yasuda, and K Tanaka for their kind support with histological assessment, immunohistochemical assessment, and real-time RT-PCR assessment. We would like to thank Editage (www.editage.jp) for English language editing.

Author contributions

TF, KO, and TN conceived and designed the study; acquired, analyzed, and interpreted the data; and drafted and critically revised the manuscript. RK conceived and designed the study and drafted and critically revised the manuscript. KS acquired, analyzed, and interpreted the data and drafted and revised the manuscript. TO, RY, KT, SI, RN acquired, analyzed, and interpreted the data. All authors read and approved the final manuscript.

Funding

No funding was received for this study.

Data availability

The datasets generated and/or analysed during the current study are available in the NCBI GenBank database, with the following accession numbers: NM_017008.3, NM_012929.1, NM_013140.1, NM_133530.1, NM_013059.3, XM_017596552.3, XM_017594791.3, NM_001287114.1, XM_006235872.3, NM_001013062.3.

Declarations

Ethics approval and consent to participate

This study was approved by the Institutional Animal Care and Use Committee (Permission number: P180609) and carried out according to the Kobe University Animal Experimentation Regulation.

Consent for publication

Not applicable.

Competing interests

The authors declare no competing interests.

Author details

[1]Department of Orthopaedic Surgery, Kobe University Graduate School of Medicine, 7-5-1, Kusunoki-cho, Chuo-ku, Kobe 650-0017, Japan
[2]Department of Rehabilitation Science, Graduate School of Health Sciences, Kobe University, Kobe, Japan
[3]Department of Orthopaedic Surgery, Hyogo Prefectural Nishinomiya Hospital, Nishinomiya, Japan

Received: 8 January 2024 / Accepted: 17 October 2024
Published online: 29 October 2024

References

1. Zura R, Xiong Z, Einhorn T, Watson JT, Ostrum RF, Prayson MJ, et al. Epidemiology of fracture Nonunion in 18 human bones. JAMA Surg. 2016;151:e162775.
2. Giannoudis PV, Einhorn TA, Marsh D. Fracture healing: the diamond concept. Injury. 2007;38(Suppl 4):S3–6.
3. Giannoudis PV, Einhorn TA, Schmidmaier G, Marsh D. The diamond concept–open questions. Injury. 2008;39(Suppl 2):S5–8.
4. Heckman JD, Ryaby JP, McCabe J, Frey JJ, Kilcoyne RF. Acceleration of tibial fracture-healing by non-invasive, low-intensity pulsed ultrasound. J Bone Joint Surg Am. 1994;76:26–34.
5. Govender S, Csimma C, Genant HK, Valentin-Opran A, Amit Y, Arbel R, et al. Recombinant human bone morphogenetic protein-2 for treatment of open tibial fractures: a prospective, controlled, randomized study of four hundred and fifty patients. J Bone Joint Surg Am. 2002;84:2123–34.
6. Kim SJ, Park HS, Lee DW, Lee JW. Short-term daily teriparatide improve postoperative functional outcome and fracture healing in unstable intertrochanteric fractures. Injury. 2019;50:1364–70.
7. Harrison A, Lin S, Pounder N, Mikuni-Takagaki Y. Mode & mechanism of low intensity pulsed ultrasound (LIPUS) in fracture repair. Ultrasonics. 2016;70:45–52.
8. Sant'Anna EF, Leven RM, Virdi AS, Sumner DR. Effect of low intensity pulsed ultrasound and BMP-2 on rat bone marrow stromal cell gene expression. J Orthop Res. 2005;23:646–52.
9. Sena K, Leven RM, Mazhar K, Sumner DR, Virdi AS. Early gene response to low-intensity pulsed ultrasound in rat osteoblastic cells. Ultrasound Med Biol. 2005;31:703–8.
10. Barzelai S, Sharabani-Yosef O, Holbova R, Castel D, Walden R, Engelberg S, et al. Low-intensity ultrasound induces angiogenesis in rat hind-limb ischemia. Ultrasound Med Biol. 2006;32:139–45.
11. Oe K, Ueha T, Sakai Y, Niikura T, Lee SY, Koh A, et al. The effect of transcutaneous application of carbon dioxide CO_2 on skeletal muscle. Biochem Biophys Res Commun. 2011;407:148–52.
12. Sakai Y, Miwa M, Oe K, Ueha T, Koh A, Niikura T, et al. A novel system for transcutaneous application of carbon dioxide causing an artificial Bohr effect in the human body. PLoS ONE. 2011;6:e24137.
13. Koga T, Niikura T, Lee SY, Okumachi E, Ueha T, Iwakura T, et al. Topical cutaneous CO_2 application by means of a novel hydrogel accelerates fracture repair in rats. J Bone Joint Surg Am. 2014;96:2077–84.
14. Kumabe Y, Fukui T, Takahara S, Kuroiwa Y, Arakura M, Oe K, et al. Percutaneous CO_2 treatment accelerates bone generation during distraction osteogenesis in rabbits. Clin Orthop Relat Res. 2020;478:1922–35.

15. Kuroiwa Y, Fukui T, Takahara S, Lee SY, Oe K, Arakura M, et al. Topical cutaneous application of CO_2 accelerates bone healing in a rat femoral defect model. BMC Musculoskelet Disord. 2019;20:237.
16. Bonnarens F, Einhorn TA. Production of a standard closed fracture in laboratory animal bone. J Orthop Res. 1984;2:97–101.
17. Clatworthy MG, Clark DI, Gray DH, Hardy AE. Reamed versus unreamed femoral nails. A randomised, prospective trial. J Bone Joint Surg Br. 1998;80:485–9.
18. Kooistra BW, Dijkman BG, Busse JW, Sprague S, Schemitsch EH, Bhandari M. The radiographic union scale in tibial fractures: reliability and validity. J Orthop Trauma. 2010;24(Suppl 1):S81–6.
19. Fiset S, Godbout C, Crookshank MC, Zdero R, Nauth A, Schemitsch EH. Experimental validation of the Radiographic Union Score for tibial fractures (RUST) using Micro-computed Tomography scanning and Biomechanical Testing in an in-vivo rat model. J Bone Joint Surg Am. 2018;100:1871–8.
20. Tawonsawatruk T, Hamilton DF, Simpson AH. Validation of the use of radiographic fracture-healing scores in a small animal model. J Orthop Res. 2014;32:1117–9.
21. Cooke ME, Hussein AI, Lybrand KE, Wulff A, Simmons E, Choi JH, et al. Correlation between RUST assessments of fracture healing to structural and biomechanical properties. J Orthop Res. 2018;36:945–53.
22. Allen HL, Wase A, Bear WT. Indomethacin and aspirin: effect of nonsteroidal anti-inflammatory agents on the rate of fracture repair in the rat. Acta Orthop Scand. 1980;51:595–600.
23. Vanchinathan V, Mirzamani N, Kantipudi R, Schwartz EJ, Sundram UN. The vascular marker CD31 also highlights histiocytes and histiocyte-like cells within cutaneous tumors. Am J Clin Pathol. 2015;143:177–85.
24. Kusumbe AP, Ramasamy SK, Adams RH. Coupling of angiogenesis and osteogenesis by a specific vessel subtype in bone. Nature. 2014;507:323–8.
25. Melikian N, Seddon MD, Casadei B, Chowienczyk PJ, Shah AM. Neuronal nitric oxide synthase and human vascular regulation. Trends Cardiovasc Med. 2009;19:256–62.
26. Lawler PR, Lawler J. Molecular basis for the regulation of angiogenesis by thrombospondin-1 and – 2. Cold Spring Harb Perspect Med. 2012;2:a006627.
27. Livak KJ, Schmittgen TD. Analysis of relative gene expression data using real-time quantitative PCR and the 2(-Delta Delta C(T)) method. Methods. 2001;25:402–8.
28. Duarte LR. The stimulation of bone growth by ultrasound. Arch Orthop Trauma Surg. 1983;101:153–9.
29. Yang KH, Parvizi J, Wang SJ, Lewallen DG, Kinnick RR, Greenleaf JF, et al. Exposure to low-intensity ultrasound increases aggrecan gene expression in a rat femur fracture model. J Orthop Res. 1996;14:802–9.
30. Azuma Y, Ito M, Harada Y, Takagi H, Ohta T, Jingushi S. Low-intensity pulsed ultrasound accelerates rat femoral fracture healing by acting on the various cellular reactions in the fracture callus. J Bone Min Res. 2001;16:671–80.
31. Takayama T, Suzuki N, Ikeda K, Shimada T, Suzuki A, Maeno M, et al. Low-intensity pulsed ultrasound stimulates osteogenic differentiation in ROS 17/2.8 cells. Life Sci. 2007;80:965–71.
32. Cheung WH, Leung KS, Chow SK. Ultrasound and fragility fracture: is there a role? Injury. 2016;47(Suppl 1):S39–42.
33. Mukai S, Ito H, Nakagawa Y, Akiyama H, Miyamoto M, Nakamura T. Transforming growth factor-beta1 mediates the effects of low-intensity pulsed ultrasound in chondrocytes. Ultrasound Med Biol. 2005;31:1713–21.
34. Sekino J, Nagao M, Kato S, Sakai M, Abe K, Nakayama E, et al. Low-intensity pulsed ultrasound induces cartilage matrix synthesis and reduced MMP13 expression in chondrocytes. Biochem Biophys Res Commun. 2018;506:290–7.
35. Hartmann BR, Bassenge E, Hartmann M. Effects of serial percutaneous application of carbon dioxide in intermittent claudication: results of a controlled trial. Angiology. 1997;48:957–63.
36. Piazzolla LP, Louzada LL, Scoralick FM, Martins ME, de Sousa JB. Preliminary experience with carbon dioxide therapy in the treatment of pressure ulcers in a bedridden elderly patient. J Am Geriatr Soc. 2012;60:378–9.
37. Oda T, Niikura T, Fukui T, Oe K, Kuroiwa Y, Kumabe Y, et al. Transcutaneous CO_2 application accelerates fracture repair in streptozotocin-induced type I diabetic rats. BMJ Open Diabetes Res Care. 2020;8:e001129.
38. Mansjur KQ, Kuroda S, Izawa T, Maeda Y, Sato M, Watanabe K, et al. The effectiveness of human parathyroid hormone and low-intensity pulsed Ultrasound on the Fracture Healing in Osteoporotic. Bones Ann Biomed Eng. 2016;44:2480–8.
39. Warden SJ, Komatsu DE, Rydberg J, Bond JL, Hassett SM. Recombinant human parathyroid hormone (PTH 1–34) and low-intensity pulsed ultrasound have contrasting additive effects during fracture healing. Bone. 2009;44:485–94.
40. Dimitriou R, Tsiridis E, Giannoudis PV. Current concepts of molecular aspects of bone healing. Injury. 2005;36:1392–404.
41. Maruyama M, Rhee C, Utsunomiya T, Zhang N, Ueno M, Yao Z, et al. Modulation of the Inflammatory Response and Bone Healing. Front Endocrinol (Lausanne). 2020;11:386.
42. Hankenson KD, Dishowitz M, Gray C, Schenker M. Angiogenesis in bone regeneration. Injury. 2011;42:556–61.
43. Marsell R, Einhorn TA. The biology of fracture healing. Injury. 2011;42:551–5.
44. Wang FS, Kuo YR, Wang CJ, Yang KD, Chang PR, Huang YT, et al. Nitric oxide mediates ultrasound-induced hypoxia-inducible factor-1alpha activation and vascular endothelial growth factor-A expression in human osteoblasts. Bone. 2004;35:114–23.
45. D'Arcangelo D, Facchiano F, Barlucchi LM, Melillo G, Illi B, Testolin L, et al. Acidosis inhibits endothelial cell apoptosis and function and induces basic fibroblast growth factor and vascular endothelial growth factor expression. Circ Res. 2000;86:312–8.
46. Baum O, Da Silva-Azevedo L, Willerding G, Wöckel A, Planitzer G, Gossrau R, et al. Endothelial NOS is main mediator for shear stress-dependent angiogenesis in skeletal muscle after prazosin administration. Am J Physiol Heart Circ Physiol. 2004;287:H2300–8.
47. Aguirre J, Buttery L, O'Shaughnessy M, Afzal F, Fernandez de Marticorena I, Hukkanen M, et al. Endothelial nitric oxide synthase gene-deficient mice demonstrate marked retardation in postnatal bone formation, reduced bone volume, and defects in osteoblast maturation and activity. Am J Pathol. 2001;158:247–57.
48. Shen G. The role of type X collagen in facilitating and regulating endochondral ossification of articular cartilage. Orthod Craniofac Res. 2005;8:11–7.
49. Behonick DJ, Xing Z, Lieu S, Buckley JM, Lotz JC, Marcucio RS, et al. Role of matrix metalloproteinase 13 in both endochondral and intramembranous ossification during skeletal regeneration. PLoS ONE. 2007;2:e1150.
50. Li X, Li J, Cheng K, Lin Q, Wang D, Zhang H, et al. Effect of low-intensity pulsed ultrasound on MMP-13 and MAPKs signaling pathway in rabbit knee osteoarthritis. Cell Biochem Biophys. 2011;61:427–34.
51. Wang X, Manner PA, Horner A, Shum L, Tuan RS, Nuckolls GH. Regulation of MMP-13 expression by RUNX2 and FGF2 in osteoarthritic cartilage. Osteoarthritis Cartilage. 2004;12:963–73.
52. Nakashima K, Zhou X, Kunkel G, Zhang Z, Deng JM, Behringer RR, et al. The novel zinc finger-containing transcription factor osterix is required for osteoblast differentiation and bone formation. Cell. 2002;108:17–29.
53. Fung CH, Cheung WH, Pounder NM, de Ana FJ, Harrison A, Leung KS. Effects of different therapeutic ultrasound intensities on fracture healing in rats. Ultrasound Med Biol. 2012;38:745–52.
54. ter Haar G. Therapeutic applications of ultrasound. Prog Biophys Mol Biol. 2007;93:111–29.
55. Wang SJ, Lewallen DG, Bolander ME, Chao EY, Ilstrup DM, Greenleaf JF. Low intensity ultrasound treatment increases strength in a rat femoral fracture model. J Orthop Res. 1994;12:40–7.

Publisher's note